

- Levin, I. W., Thompson, T. E., Barenholz, Y. B., & Huang, C. (1985) *Biochemistry* 24, 6282-6286.
- Levitt, M. (1974) *J. Mol. Biol.* 82, 393-420.
- Mabrey, S., & Sturtevant, J. M. (1976) *Proc. Natl. Acad. Sci. U.S.A.* 73, 3862-3866.
- Mason, J. T., & Huang, C. (1981) *Lipids* 16, 604-608.
- Mason, J. T., Huang, C., & Biltonen, R. L. (1981) *Biochemistry* 20, 6086-6092.
- McDaniel, R. V., McIntosh, T. J., & Simon, S. A. (1983) *Biochim. Biophys. Acta* 731, 97-108.
- McIntosh, T. J., Simon, S. A., Ellington, J. C., Jr., & Porter, N. A. (1984) *Biochemistry* 23, 4038-4044.
- Pascher, I., & Sundell, S. (1986) *Biochim. Biophys. Acta* 855, 68-78.
- Pascher, I., Sundell, S., Ebil, H., & Harlos, K. (1986) *Chem. Phys. Lipids* 39, 53-64.
- Pauling, L. (1960) in *The Nature of the Chemical Bond*, 3rd ed., Cornell University Press, Ithaca, NY.
- Pearson, R. H., & Pascher, I. (1979) *Nature (London)* 281, 499-501.
- Ranck, J. L., & Tocanne, J. F. (1982) *FEBS Lett.* 143, 171-174.
- Ranck, J. L., Keira, T., & Luzzati, V. (1977) *Biochim. Biophys. Acta* 488, 431-441.
- Ruocco, M. J., Siminovitch, D. J., & Griffin, R. G. (1985) *Biochemistry* 24, 2406-2411.
- Serrallach, E. N., Dijkman, R., de Haas, G. H., & Shipley, G. G. (1983) *J. Mol. Biol.* 170, 155-174.
- Silvius, J. R., Read, B. D., & McElhaney, R. N. (1979) *Biochim. Biophys. Acta* 555, 175-178.
- Wu, W., Chong, P. L., & Huang, C. (1985) *Biophys. J.* 47, 237-242.
- Zaccai, G., Büldt, G., Seelig, A., & Seelig, J. (1979) *J. Mol. Biol.* 134, 683-706.

High-Resolution ^1H NMR Study of the Solution Structure of Alamethicin[†]

Gennaro Esposito,[†] John A. Carver,[§] Jonathan Boyd, and Iain D. Campbell*

Department of Biochemistry, University of Oxford, OX1 3QU Oxford, U.K.

Received July 25, 1986; Revised Manuscript Received October 17, 1986

ABSTRACT: A ^1H NMR study of the peptide alamethicin, which forms voltage-gated ion channels in membranes, is described. The molecule was studied in methanol as a function of temperature and pH. A complete assignment of the spectra is given, including several stereospecific assignments. Alamethicin was found to have a structure substantially similar to the crystal although, in solution, the C-terminal dipeptide adopts a somewhat extended conformation. The overall conformation was insensitive to the ionization of the side chain of the only ionizable group, Glu-18.

Alamethicin is a linear icosapeptide that has antibiotic activity (Payne et al., 1970). It is extracted from the fungus *Trichoderma viride* as a mixture of related compounds, of which the main component has the following sequence (Gisin et al., 1977): Ac-Aib-Pro-Aib-Ala-Aib-Ala-Gln-Aib-Val-Aib-Gly-Leu-Aib-Pro-Val-Aib-Aib-Glu-Gln-Phol, where Aib¹ is α -aminoisobutyric acid [$(\text{CH}_3)_2\text{C}(\text{NH}_2)\text{CO}_2\text{H}$] and Phol is phenylalaninol, the α -amino alcohol derivative of phenylalanine.

Alamethicin forms voltage-gated ion channels in membranes (Mueller & Rudin, 1968; Fringeli & Fringeli, 1979; Lau & Chan, 1976; Banerjee et al., 1985). Two main classes of models have been proposed for the way in which this gated channel operates. These are the conformational change models and the helix dipole models. For example, Hall et al. (1984) proposed a conformational transition between a bent structure and a linear one as the basic gating event. This model is related to the one proposed by Fox and Richards (1982) although the "open" and "closed" states are not the same. Those models involving the helix dipole moment include those where

the helix "flips" across the membrane and those where the helices in the channel move with respect to each other (Boheim et al., 1983; Mathew & Balaram, 1983; Edmonds, 1985).

These proposals for the action of the channel remain speculative since the structure of alamethicin in the lipid bilayer is unknown. In fact, there is conflicting evidence on its structure in the membrane since both an α -helical conformation (Boheim & Kolb, 1978) and a membrane-spanning β structure (Fringeli & Fringeli, 1979) have been reported.

Structural studies have, however, been carried out in various other solvents. The X-ray structure of alamethicin, crystallized from methanol (Fox & Richards, 1982), is predominantly helical. After the initial α -helix segment, Pro-14 introduces a bend that shifts the axis of the subsequent 3_{10} helix formed by the C-terminal residues. Circular dichroism studies (McMullen et al., 1971; Jung et al., 1975) showed a helix content ranging from 20% to 45% in a variety of organic solvents.

[†] This is a contribution from the Oxford Enzyme Group, which is supported by SERC.

* Author to whom correspondence should be addressed.

[†] Permanent address: Eniricerche spa, 32 00015 Monterotondo (Roma), Italy.

[§] Present address: Department of Biochemistry, University of Adelaide, Adelaide, South Australia 5000, Australia.

¹ Abbreviations: NMR, nuclear magnetic resonance; 2D, two dimensional; DQF COSY, double quantum filtered correlation spectroscopy; NOESY, nuclear Overhauser enhancement spectroscopy; NOE, nuclear Overhauser effect; CYCLOPS, cyclic ordered phase scheme; ppm, parts per million; Hz/pt, hertz per point; Aib, α -aminoisobutyric acid; Phol, L-phenylalaninol; TSP, sodium 2,2,3,3-tetradeuterio-3-(trimethylsilyl)propionate; HPLC, high-performance liquid chromatography; rms, root mean square.

Early NMR studies (Jung et al., 1975; Martin & Williams, 1976) contributed to the determination of the correct primary structure. Later Davis and Gisin (1981) used 600-MHz ^1H NMR to assign many of the resonances. From the different isotopic exchange rates observed for the backbone NH's, a rigid α -helical structure was inferred for the N-terminal portion of the molecule (3–10), with a more flexible C-terminus.

Alamethicin has also been studied in methanol and in water by both one- and two-dimensional (2D) NMR techniques (Banerjee et al., 1983; Banerjee & Chan, 1983; Davis & Bax, 1985). From analysis of coupling constants and relaxation parameters, Banerjee et al. (1983) inferred a head to head dimeric association of the peptide via intermolecular hydrogen bonds between groups on residues 15–20, arranged in an extended parallel β pleated structure.

We present a ^1H 2D NMR study of purified alamethicin in methanol at 500 and 300 MHz. The resonances, including the Aib residues, are assigned. Characteristic NOE patterns for a helix were observed, and it was possible to make detailed comparisons of the structure of the molecule in solution with the structure described by Fox and Richards (1982). Contrary to previous reports (Banerjee et al., 1983), the conformation of the molecule in solution was found to be largely similar to the crystal structure.

MATERIALS AND METHODS

Alamethicin from two sources was used: a gift from Upjohn Co. (Kalamazoo, MI) and a sample purchased from PHLS (Porton, Down, U.K.). The crude product was purified by HPLC with a preparative column (Partisil-10 ODS-3, Whatman, Maidstone, U.K.) according to the procedure of Gisin et al. (1981) with high-purity CH_3OH (Fisons), Et_3NH , and AcOH (Sigma) although a slightly different pH value (4.85) of the eluent was used to obtain better separation. After the fraction of interest was collected, the methanol was evaporated and the remaining aqueous solution was repeatedly freeze-dried. The purified sample was dissolved in CD_3OH (MSD) (5–6 mM). The pH values reported are the uncorrected meter readings (pH*).

^1H NMR spectra were mainly recorded at 500 MHz with a spectrometer assembled in this laboratory (Oxford Instruments magnet and GE/Nicolet 1280 computer). Experiments were performed mainly at 24.5 °C but also at –5 and 39 °C.

Double quantum filtered (DQF) COSY spectra were obtained by using the pulse sequence described by Piantini et al. (1982). Phase cycles that select the N peaks (Wokaun & Ernst, 1977; Shaka & Freeman, 1983) were used; consequently the data from this experiment were not phase sensitive. CYCLOPS (Hoult & Richards, 1975) was superimposed on the basic eight-step phase cycle, resulting in a minimum of 32 scans for the complete phase-cycling scheme. The intense OH resonance was reduced by irradiation only during the recycling delay t_0 (1 s) to avoid Bloch–Siegert shifts (Wider et al., 1983). For each t_1 increment, 96 or 128 transients were collected, and a sweep width of ± 2500 Hz was used for both the F_1 and F_2 dimensions. Prior to complex Fourier transformation, the initial 512×4096 data matrix was filtered by using both sine wave and double-exponential multiplication in t_2 and sine wave multiplication in t_1 . The latter dimension was zero filled twice to obtain a square $2\text{K} \times 2\text{K}$ real matrix.

Phase-sensitive NOESY spectra were acquired by using the method described by States et al. (1982). Two different values for the mixing time t_m were used (190 and 294 ms). A random variation of t_m , Δ , of $0.05t_m$ was introduced, to minimize the contribution of the coherent magnetization transfers between

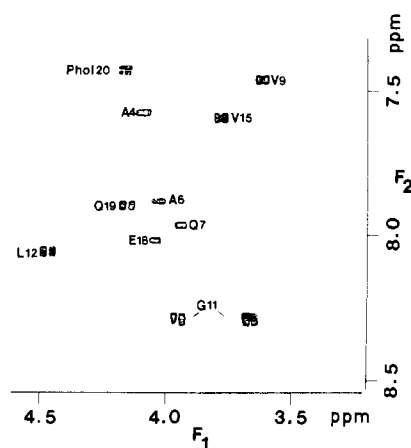


FIGURE 1: ^1H 500-MHz double quantum filtered COSY spectrum of alamethicin in CD_3OH ($T = 39^\circ\text{C}$, $\text{pH}^* 9.1$). The region shown corresponds to the NH- α -CH cross peaks.

scalar coupled nuclei (Macura et al., 1982). In the NOESY experiments solvent presaturation was achieved by continuous selective irradiation during both t_0 (1 s) and $t_m + \Delta$. The number of transients collected for each t_1 increment was 192 (96 + 96). The phase corrections of the 1D spectrum, acquired by using the same experimental conditions, were used for phasing after the first Fourier transform. The 512×2048 data matrix was zero filled once in t_1 . In the final $1\text{K} \times 1\text{K}$ real matrix the digital resolution was 4.78 Hz/pt in both dimensions. No resolution enhancement was applied to avoid artifacts in the evaluation of the integrated intensities. Integrals of diagonal and cross peaks were determined from cross sections parallel to F_1 .

Experiments involving 1D spectra, including temperature and pH* dependences, were acquired mainly with a Bruker WH 300 instrument. Simulations of the 300-MHz spectra were performed by using the PANIC program of the Bruker software package. Identification of the spectral lines in crowded regions was achieved, when necessary, by selective decoupling difference spectroscopy. The results of the simulations were also checked by comparing the experimental and calculated spectra at 500 and 300 MHz. J values were measured from 1D experiments at 500 MHz so that high digital resolution could be achieved.

Crystal structure distances and dihedral angles were evaluated by using a Evans and Sutherland PS300 molecular graphics system and the coordinates of Fox and Richards (1982).

RESULTS AND DISCUSSION

The results listed below depend on the analysis of 500-MHz ^1H NMR 2D double quantum filtered COSY spectra (typical spectrum shown in Figure 1) and phase-sensitive 2D NOESY spectra (typical spectrum in Figure 2) collected at two values of pH* (6.1 and 9.1). These values were chosen because they correspond, in methanol, to pH values below and above the pK_a of Glu-18. Further information was obtained from pH titrations, amide proton exchange rates, and temperature dependence of shifts.

Table I lists the assignments of alamethicin in CD_3OH at 24.5 °C and at both pH* 6.1 and pH* 9.1. Figure 2 shows the low-field region of the 2D contour plot obtained from a phase-sensitive NOESY experiment with a mixing time of 300 ms at pH* 6.1; sequential NOE connectivities between NH protons are traced out. This spectrum was recorded at –5 °C to enhance the observed NOEs. Figure 3 summarizes the spatial connectivities inferred from the NOESY cross peaks.

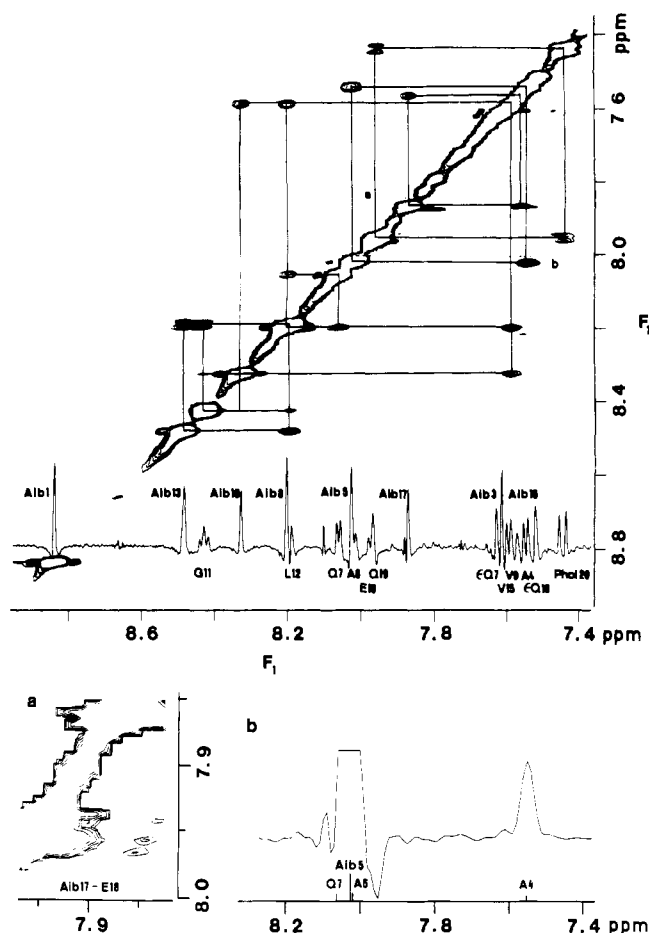


FIGURE 2: ^1H 500-MHz phase-sensitive NOESY spectrum of alamethicin in CD_3OH ($T = -5.5^\circ\text{C}$, $\text{pH}^* 6.1$); contour plot of the low-field region. The sequential NH-NH connectivities visible at this level of contours are traced out. The same pattern was observed at higher temperatures (24.5 and 39°C), but the intensities of the cross peaks decreased. In the boxed regions the Aib-17-Glu-18, the Aib-5-Ala-6, and the Ala-6-Gln-7 connectivities should appear. The former can be seen at higher contour level (insert a). The latter two cannot be detected since, at this temperature, they are obscured in the diagonal (the positions of the amide resonances of Ala-6 and Gln-7 are, however, marked in insert b). These cross peaks are resolved at higher temperature.

Two different types of NOE are presented in the two quadrants of this figure. The upper shows only the intraresidue connectivities, while the lower shows only the interresidue ones. The results were similar at both the pH^* values investigated. Most of the observed interresidue NOE connectivities are consistent with those expected for helical structures (Wüthrich et al., 1984).

Assignments. Spectral assignments, including some stereospecific assignments (see Appendix), are listed in Table I. It should be realized that there is an interrelationship between such assignments and structural conclusions reached with NMR.

First-stage assignment, to amino acid type, was achieved by identification of the spin systems using the scalar coupling connectivities in DQF COSY spectra (Wider et al., 1982). Second-stage assignments, to particular amino acids, can be achieved immediately for those that only appear once in the sequence, i.e., Gly-11, Leu-12, and Phol-20. All the remaining residues were assigned by using the sequential assignment procedures outlined by Wagner and Wüthrich (1982).

The assignment of all eight Aib residue amide protons in alamethicin has been achieved by using sequential NOE connectivities. This residue has previously been difficult to

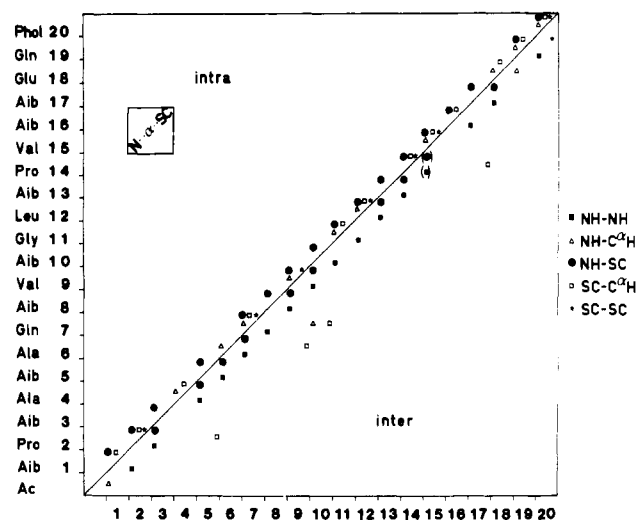


FIGURE 3: Summary of the intra- (upper left) and interresidue (lower right) NOESY connectivities of alamethicin in CD_3OH at $T = 24.5^\circ\text{C}$ at both the pH^* conditions investigated. The insert shows, on a larger scale, the coordinates of the three different types of protons linked by NOESY connectivities [backbone NH, C^αH , and side chain (SC)]. Different symbols are used for each pairwise interaction. The *pro-S* and the *pro-R* β -methyls of the Aib residues are considered sterically equivalent to side-chain and α protons, respectively. The *pro-S* α proton of Gly-11 is considered as a side chain. The δ protons of Pro residues are considered equivalent to NH's. The SC-SC interresidue connectivity between Gln-19 and Phol-20 refers to the ϵ -NH aromatic ortho proton connectivity (see text and Appendix). In cases where overlap of resonances caused ambiguities, the corresponding connectivities are displayed in parentheses.

assign (Martin & Williams, 1976; Davis & Gisin, 1981; Banerjee et al., 1983) because the absence of an α -CH makes it impossible to trace through-bond connectivities. The Aib residues are, however, crucial in determining the structure of alamethicin and related compounds (Balaram, 1983).

The ϵ -amide protons of Gln-7 and Glu-19 give rise to strong cross peaks in the NOESY spectrum, which are due to chemical exchange. These resonances were distinguished by NOE effects, observed at $\text{pH}^* 9.1$, between the aromatic ortho protons of Phol-20 and the highest field amide proton resonance.

The assignment of the glutamate and glutamine spin systems depended also on an analysis of the effects of varying pH^* as outlined below.

Effects of pH^* . The pK_a of the single carboxyl group of alamethicin, the Glu-18 side chain, is expected to increase in methanol compared to water (Bates, 1971). By use of the chemical shift of the resonances as an indicator and the uncorrected pH meter reading, the measured pK_a in methanol was 7.75.

As shown in Table I, no major changes were found in chemical shifts or coupling constants between $\text{pH}^* 6.1$ and $\text{pH}^* 9.1$. The main effects detected on decreasing the pH^* to 6.1 were an upfield shift of two backbone NH signals and the Gln-19 anti NH (Figure 4) and a downfield shift of some resonances around 2.4–2.5 ppm (from the CH_2 of Glu-18—see below). One of the upfield-shifted backbone NH resonances if from Phol-20, and the other is attributed to a Gln/Glu-type residue.

The alamethicin spectrum contains three ABFGQX spin systems arising from Gln-7, Gln-19, and Glu-18. Gln-7 was assigned from sequential NOESY results. The resonances of the remaining two residues are well separated at basic pH^* (see Table I), but their NH's nearly overlap at $\text{pH}^* 6.1$. The corresponding α -CH's do not show significant pH-induced

Table I: Chemical Shifts of Alamethicin in CD₃OH (*T* = 24.5 °C)^a

pH* 6.1			pH* 9.1			pH* 6.1			pH* 9.1		
<i>N</i> -Ac		2.067			2.060	Leu-12	NH	8.109			8.096
Aib-1	NH	8.679			8.675		α	4.45			4.46
	β	1.49; 1.55			1.48; –		β	1.95; 1.63			1.94; 1.62
Pro-2	α	4.246			4.244		γ	1.91			1.89
	β	<i>pro-S</i> , 2.32; <i>pro-R</i> , 1.83			<i>pro-S</i> , 2.35; <i>pro-R</i> , 1.81		δ	0.936; 0.914			0.932; 0.910
	γ	<i>pro-S</i> , 2.07; <i>pro-R</i> , 1.97			<i>pro-S</i> , 2.06; <i>pro-R</i> , 1.98	Aib-13	NH	8.370			8.338
	δ	<i>pro-R</i> , 3.93; <i>pro-S</i> , 3.51			<i>pro-R</i> , 3.96; <i>pro-S</i> , 3.49		β	<i>pro-S</i> , 1.61; –			<i>pro-S</i> , 1.60; –
Aib-3	NH	7.613			7.614	Pro-14	α	4.373			4.365
	β	–; –			1.54; –		β	2.32; 1.81			2.32; 1.82
Ala-4	NH	7.567			7.558		γ	2.07; 2.00			2.09; 2.00
	α	4.08			4.08		δ	<i>pro-R</i> , 3.88; <i>pro-S</i> , 3.73			<i>pro-R</i> , 3.86; <i>pro-S</i> , 3.73
	β	1.495			1.492	Val-15	NH	7.589			7.589
Aib-5	NH	7.954			7.947		α	3.73			3.76
	β	<i>pro-S</i> , 1.56; –			<i>pro-S</i> , 1.56; –		β	2.34			2.34
Ala-6	NH	7.926			7.930		γ	1.071; 0.979			1.075; 0.986
	α	4.03			4.03	Aib-16	NH	7.575			7.568
	β	1.531			1.531		β	1.55; 1.52			1.55; –
Gln-7	NH	7.992			7.995	Aib-17	NH	7.785			7.784
	α	3.92			3.94		β	<i>pro-S</i> , 1.55; –			<i>pro-S</i> , 1.56; –
	β	2.28; 2.15			2.28; 2.13	Glu-18	NH	7.927			8.036
	γ	2.53; 2.35			2.54; 2.35		α	4.04			4.04
	ϵ -NH	syn, 6.766; anti, 7.455			syn, 6.773; anti, 7.451		β	2.29; 2.18			2.22; –
Aib-8	NH	8.078			8.088		γ	2.68; 2.50			2.49; 2.38
	β	<i>pro-S</i> , 1.61; –			<i>pro-S</i> , 1.60; –	Gln-19	NH	7.906			7.924
Val-9	NH	7.504			7.498		α	4.15			4.16
	α	3.60			3.62		β	2.04; 2.00			2.04; 1.98
	β	2.24			2.24		γ	2.33; 2.18			2.36; 2.18
	γ	<i>pro-S</i> , 1.135; <i>pro-R</i> , 1.003			<i>pro-S</i> , 1.134; <i>pro-R</i> , 0.999	Phol-20 ^b	ϵ -NH	syn, 6.641; anti, 7.342			syn, 6.629; anti, 7.486
Aib-10	NH	8.217			8.224		NH	7.354			7.458
	β	<i>pro-S</i> , 1.56; <i>pro-R</i> , 1.54			<i>pro-S</i> , 1.56; –		α	4.169			4.163
Gly-11 ^b	NH	8.335			8.344		β	<i>pro-S</i> , 2.914; <i>pro-R</i> , 2.730			<i>pro-S</i> , 2.889; <i>pro-R</i> , 2.741
	α	<i>pro-S</i> , 3.917; <i>pro-R</i> , 3.645			<i>pro-S</i> , 3.935; <i>pro-R</i> , 3.660		β'	3.628			3.628
							ortho	7.28			7.28
							meta	7.23			7.22
							para	7.15			7.14

^a In ppm using TSP as reference. In the text the nonequivalent protons are always numbered in order of decreasing chemical shift; i.e., Gly-11 α_1 represents the low-field proton. $\Delta\delta = \pm 0.001$ ppm when obtained from 1D spectra (or their simulations); $\Delta\delta = \pm 0.01$ ppm when obtained from 2D spectra. ^b Obtained by simulation.

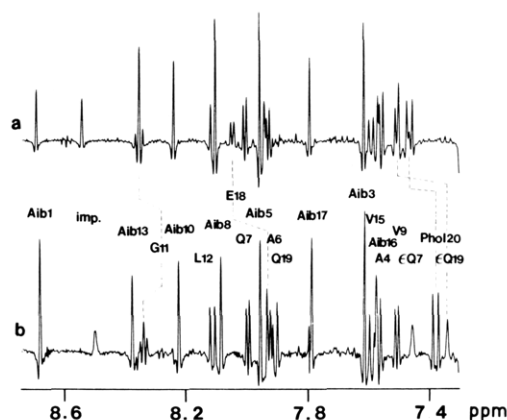


FIGURE 4: ¹H 500-MHz low-field region of alamethicin in CD₃OH at (a) pH* 9.1 and (b) 6.1 (*T* = 24.5 °C). Three NH resonances are significantly shifted upfield at neutral pH*: Glu-18, Phol-20, and Gln-19 ϵ -anti (see text).

shifts. Analysis of the DQF COSY cross peaks at the two values of pH* suggests that the α -CH at 4.04 ppm is from Glu-18, since both the β , γ -CH₂ and NH of this spin system exhibit expected titration shifts (Bundi & Wüthrich, 1979a,b). It should be noted that these assignments differ from those previously published (Davis & Gisin, 1981; Banerjee et al., 1983). The structural implications of the pH-induced shifts are discussed under Structure.

Temperature Dependence. The values of the thermal coefficients of the alamethicin amide proton shifts, obtained in CD₃OH over the range 21–40 °C, are listed in Table II. The general features are as follows:

Table II: NH Thermal Coefficients (ppb/deg) in CD₃OH^a

	pH* 6.1	pH* 9.1		pH* 6.1	pH* 9.1
Aib-1	–5.5	–4.9	Val-15	0.1	0.0
Aib-3	0.1	0.1	Aib-16	0.3	0.4
Ala-4	0.9	0.8	Aib-17	–3.0	–2.9
Aib-5	–2.2	–1.8	Glu-18	–1.7	–1.3
Ala-6	–3.1	–2.8	Gln-19	–1.8	–1.6
Gln-7	–2.2	–2.1	Phol-20	–2.2	–2.1
Aib-8	–4.5	–4.0	Gln-7		
Val-9	–3.0	–2.6	ϵ -syn	–6.1	–6.0
Aib-10	–4.1	–3.8	ϵ -anti	–6.0	–6.0
Gly-11	–3.5	–3.2	Gln-19		
Leu-12	–3.1	–2.6	ϵ -syn	–5.5	–5.4
Aib-13	–4.3	–3.7	ϵ -anti	–6.0	–6.7

^a Obtained in the range 21–40 °C.

(i) Most values of $\Delta\delta/\Delta T$ for the alamethicin NH's are small and negative (i.e., upfield shift with temperature increase). Slightly smaller values of $|\Delta\delta/\Delta T|$ are consistently detected at higher pH.

(ii) Aib-8, Aib-10, and Aib-13 have relatively large values of $|\Delta\delta/\Delta T|$. It is likely that this reflects the extent of solvent exposure of the amide protons rather than the lability of the hydrogen bonds (Ohnishi & Urry, 1969), since the $J_{\text{NH}\alpha}$ coupling constants of the neighboring residues were found to be small and constant over the temperature range studied. This interpretation is consistent with previously published isotope exchange rates (Davis & Gisin, 1981), which showed slow exchange for the 3–10 part of the sequence relative to the 11–16 portion;

(iii) The Aib-1 NH and the ϵ -NH₂ amide protons of Gln-7 and Gln-19 side chains have a very large $|\Delta\delta/\Delta T|$ (–5, –6.7

Table III: $J_{\text{NH}\alpha}$ and Corresponding Dihedral Angles for Alamethicin in CD_3OH^a

	pH*	J	ϕ	selected value		X-ray	
				ϕ	ψ	ϕ	ψ
Ala-4	9.1	5.6	31; 89; -71; -169	-71		-57	-49
	6.1	5.5	30; 90; -70; -170	-70			
Ala-6	9.1	4.7	21; 99; -64; -176	-64		-72	-36
	6.1	4.9	23; 97; -65; -175	-65			
Gln-7	9.1	5.2	27; 93; -68; -172	-68		-67	-45
	6.1	5.3	28; 92; -69; -171	-69			
Val-9	9.1	5.6	32; 88; -71; -169	-71		-69	-41
	6.1	5.4	29; 92; -70; -170	-70			
Gly-11 ^b	9.1			-69	-24	-79	-27
	6.1			-68	-23		
Leu-12	9.1	7.7	-88; -152	-88		-84	-37
	6.1	7.9	-90; -150	-90			
Val-15	9.1	7.3	-84; -156	-84		-65	-61
	6.1	8.0	-90; -150	-90			
Glu-18	9.1	5.3	26; 94; -68; -172	-68		-76	-4
	6.1	5.7	33; 87; -72; -168	-72			
Gln-19	9.1	7.1	-83; -157	-83; -157		-94	-7
	6.1	7.3	-85; -155	-85; -155			
Phol-20	9.1	9.2	-103; -136	-103; -136		-123	59
	6.1	9.3	-107; -133	-107; -133			

^a J in Hz, angles in deg. $\Delta J = \pm 0.2$ Hz. The dihedral angles were calculated by using the calibration of Pardi et al. (1984). ^b See Table V.

ppb), suggesting that these groups are exposed and not involved in H bonds.

(iv) Residues Aib-3-Ala-4 and Val-15-Aib-16 show zero or very small positive $\Delta\delta/\Delta T$. This could be due to the presence of a Pro residue immediately before each of the above pairs.

Structure. A description of the structure of alamethicin in methanol, as determined by NMR, can now be given. It is divided into four subsections which describe different regions of the molecule.

(i) *Regular Helix Regions (Ala-4-Aib-10, Aib-16-Glu-18).* Most of the $J_{\text{NH}\alpha}$ coupling constants have values that correspond to helices (Pardi et al., 1984). Table III lists their values, along with the values of the corresponding angles. When small values of $J_{\text{NH}\alpha}$ (≤ 5.5 Hz) occur, the observation of a sequential network of NH-NH NOESY connectivities and of a number of additional "diagnostic" NOEs ($\beta_i\text{-NH}_{i+1}$, $\alpha_i\text{-}\beta_{i+3}$, $\alpha_i\text{-NH}_{i+3}$) demonstrates the presence of a helical structure (Wüthrich et al., 1984). The ϕ value corresponding to a right-handed helix is selected in Table III, since the other possibilities would not be consistent with the observed regularity of the NOEs. The selected values are very close to the corresponding values obtained for the crystal structure of alamethicin (also listed in Table III), and they fall within the statistical range observed for α helices in proteins, $\langle\phi\rangle = -65 \pm 6$ (Chothia, 1984). The possibility of 3_{10} right-handed helix cannot be ruled out, although both the experimental ϕ values and the regular network of the $\beta_i\text{-NH}_{i+1}$ contacts (shorter in α helices) suggest an α_R -type helical structure for the Ala-4-Aib-10 and Aib-16-Glu-18 portions.

(ii) *Pro-2 and Pro-14.* The close contacts between the ring protons of Pro-2 with the Aib-1 NH, Aib-3 NH, and Aib-5 CH_3 protons lead to the conclusion that the Aib-1-Pro-2 peptide bond is trans and that ψ_1 and ψ_2 angles have nearly helical values (Wüthrich et al., 1984). Similar conclusions are reached from the observed NOEs of the resonances of the ring protons of Pro-14 to the Aib-13 NH, Aib-13 $\beta\text{-CH}_3$, and Aib-17 $\beta\text{-CH}_3$ resonances. The unusual amide thermal coefficients for the two residues next to both prolines (Table II) must also reflect such similarity. Thus both prolyl residues of alamethicin in methanol appear to be in helical regions. There are, however, some deviations, especially for ψ_3 and ψ_{15} , which would explain the absence of NH-NH NOEs between

Table IV: NH-NH Distances from NOESY Spectra^a

diagonal	cross peak	R	r	crystal structure
Ala-4	Aib-5	1.9	2.6	2.98
Aib-8	Val-9	1.1	2.9	2.75
Val-9	Aib-10	1.7	2.7	2.77
Aib-10	Gly-11	1.6	2.7	2.75
Aib-10	Val-9	1.0	2.9	2.77
Leu-12	Aib-13	3.2	2.4	2.52
Leu-12	Gly-11	2.5	2.5	2.58
Aib-16	Aib-17	1.1	2.9	3.01
Glu-18	Aib-17	1.4	2.8	2.87

^a The distances r are expressed in Å and the estimated error is ± 0.3 Å, which is the value when the error in R is 50%. R is the ratio of the integrated intensities of the cross peak to the diagonal peak. This ratio is related to the cross relaxation between the dipolar coupled nuclei (Macura et al., 1982). It was pointed out by Bodenhausen and Ernst (1982) that this ratio could be used to evaluate the exchange (or the cross-relaxation) term. The cross-relaxation term is related to the internuclear distance R and the correlation time τ_c . The correlation time was evaluated as 7.2×10^{-10} s here by assuming that the separation between the δ protons of Pro-2 is 1.77 Å. Details of the method used here to evaluate the distances will be published elsewhere (Esposito et al., unpublished results).

Aib-3 and Ala-4 and between Val-15 and Aib-16.

(iii) *Gly-11-Leu-12-Aib-13.* Values of NH-NH distances calculated from integrated NOESY intensities are given in Table IV, together with the corresponding crystal structure distances and some information on how they were calculated.

The distances listed in Table IV are consistent with the structural features inferred from a qualitative examination of the NOESY results. Closer inspection of the data shows that the amide distances between Gly-11 and Leu-12 and between Leu-12 and Aib-13 are shorter than any other in the list (2.5 and 2.4 Å, respectively). Indeed, the corresponding cross peaks in the NOESY spectra were reproducibly found to be stronger than any similar connectivity. In the case of Gly-11-Leu-12, complementary evidence can be provided from evaluation of the intervening angle ψ , using the geminal coupling constant of Gly-11 (Table V) (Barfield et al., 1976). From four different values obtained (± 23 , ± 157), only one is selected in Table III, i.e., $\psi_{11} = -23$. The NH-NH distance between Gly-11 and Leu-12 would be 3.01 Å for $\psi = 23$, a value significantly larger than the 2.50 Å predicted for $\psi_{11} = -23$. Although the experimental errors in distance evaluation by NOE are high, they are not as high as the 70% error required

Table V: Coupling Constants and Dihedral Angles of Gly-11^a

pH*	$J_{\text{NH}\alpha 1}$	θ	$J_{\text{NH}\alpha 2}$	θ	$J_{\alpha 1\alpha 2}$	
9.1	5.14	$\pm 30; \pm 129$	6.21	$\pm 8; \pm 139$	-16.62	$\delta_{\alpha 1} > \delta_{\alpha 2}$
6.1	4.56	$\pm 38; \pm 124$	6.08	$\pm 12; \pm 138$	-16.68	$\delta_{\alpha 1} > \delta_{\alpha 2}$

conventions: $\theta_L = \text{H-N-C-(pro-R)-H (L)}$; $\theta_D = \text{H-N-C-(pro-S)-H (D)}$
constraints: steric, $\theta_D = \theta_L + 120^\circ$, $\phi = \theta_L + 60^\circ$, $\phi = \theta_D - 60^\circ$; NOESY, $d_{\text{NH}\alpha 2} < d_{\text{NH}\alpha 1}$; J coupling, $\theta_{\alpha 2} < \theta_{\alpha 1}$

combinations						combinations					
pH*	θ_L	ϕ	θ_D	ϕ	ϕ_{av}	pH*	θ_L	ϕ	θ_D	ϕ	ϕ_{av}
9.1	8	68	129	69	68.5	6.1	12	72	124	64	68
	-129	-69	-8	-68	-68.5		-124	-64	-12	-72	-68

^a J values in Hz; θ and ϕ values in deg. θ_D and θ_L are the dihedral angles formed respectively by the D (*pro-S*) and the L (*pro-R*) protons with the N vicinal proton. $d_{\text{NH}\alpha i}$ is the distance between the NH and the corresponding proton. All the coupling constants were obtained by simulation (rms = 0.005). The θ values were computed by using the equation reported by De Marco et al. (1978). Only the combinations listed, corresponding to the two possible stereospecific assignments of the Gly-11 α protons, meet all the constraints.

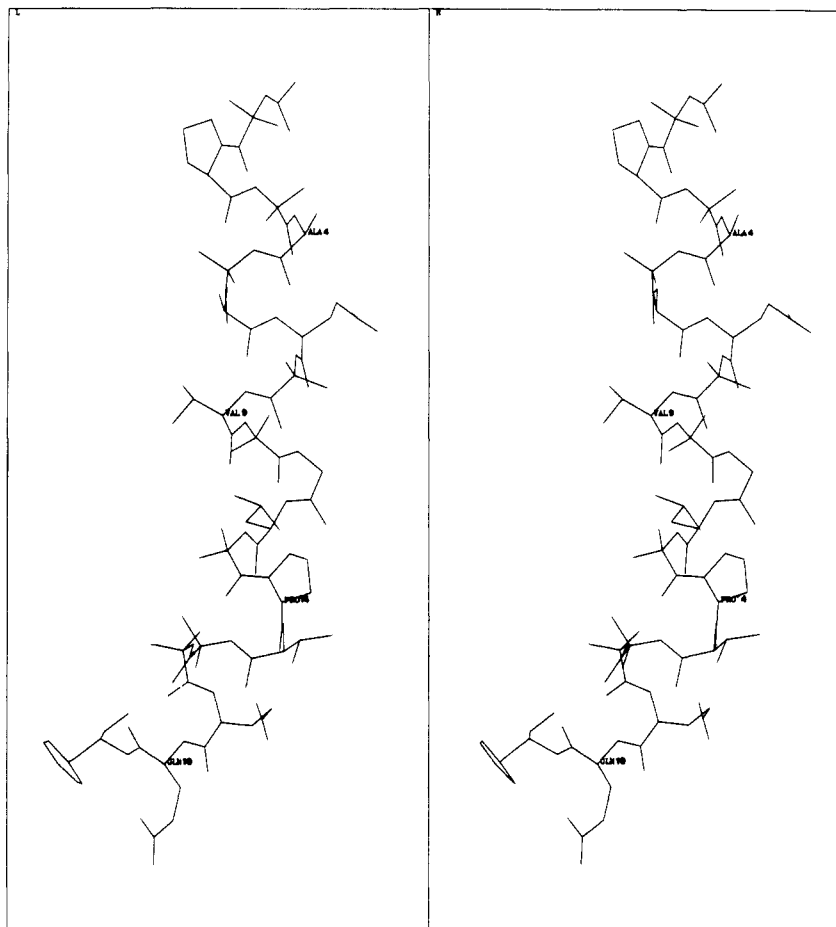


FIGURE 5: Stereo diagram of a structure of alamethicin that is consistent with the NMR data. The coordinates of Fox and Richards (1982) were adjusted by using the program FRODO (Jones, 1978).

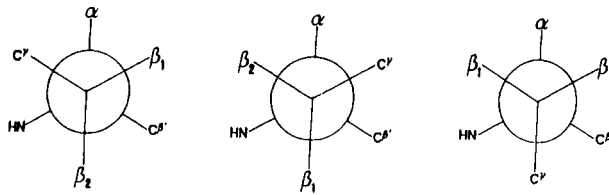
for the longer distance. Even larger distances (4–4.5 Å) would be expected for the other two values of ψ_{11} .

The close contacts mentioned above, and the selection of a single value for ϕ_{12} (Table III), consistent with the NOESY constraints, suggest a “tightening” of the helix in this region. Model inspection shows that the axis of the entire molecule might be tilted around residues 11–13 with a slight bend, reminiscent of a type I bend (Richardson, 1981). There is, however, no evidence for a reversal of the chain direction at Gly-11–Leu-12, as proposed by Hall et al. (1984).

(iv) *C-Terminal Region*. The segment Aib-16–Glu-18 appears to be a regular continuation of the helix, after the deviation introduced by Pro-14. [The degeneracy at ϕ_{15} is removed since the interatomic contacts reach the collision limit at $\phi_{15} = -120$ (Table III).] This regularity, however, breaks

at ψ_{18} , and the type of NOE connectivities detected between Glu-18 and Gln-19 (Figure 3) indicate an extended structure for the C-terminal dipeptide (Wüthrich et al., 1984). Its hydrogen bond network with the preceding residues (Fox & Richards, 1982) is thus no longer maintained in solution. The thermal coefficients of the shifts and the observed NOESY connectivities of Gln-19 and Phe-20 (Figure 3) suggest, however, that the δ_{CO} of Gln-19 is involved in hydrogen bonds with a backbone NH of the C-terminal dipeptide.

The upfield shift of the Glu-18 NH with decreasing pH* can probably be ascribed to a polarization change in the Glu-18 $\delta_{\text{CO-NH}}$ intrasidue hydrogen bond. Such effects have been observed in both oligopeptides (Bundi & Wüthrich, 1979b) and proteins (Ebina & Wüthrich, 1984). The additional upfield shifts of Phe-20 NH and Glu-19 ϵ -anti NH do not

Table VI: Phol-20 Rotamer Distribution^{a,b}


pH*	T	$J_{\alpha\beta_1}$	$J_{\alpha\beta_2}$	P_I	P_{II}	P_{III}
6.1	25	5.27	8.76	64	26	10
9.1	25	5.76	8.73	63	32	5
9.1	40	5.82	8.68	62	33	5

^a For rotamers I–III, $\beta_2 = \text{pro-R}$, $\beta_1 = \text{pro-S}$, and $\delta_{\beta_2} = \delta_{\beta_1}$. ^b T in °C, J in Hz, population in %. The values of the populations were computed by using the relationships of Haasnoot et al. (1980). The coupling constants were obtained by simulation of the experimental spectrum at 300 MHz (rms = 0.003). The most populated conformation corresponds to the crystal structure conformation. The stereospecific assignment of the β protons follows from Kobayashi and Nagai (1978).

appear to arise directly from the change in the ionization state of Glu-18. They may depend on different orientations of the δ_{CONH_2} of Gln-19.

Use of molecular models suggests that the folded conformation of the side chain of Gln-19 may also account for the rotamer population of the Phol-20 side chain (Table VI). The unusually low abundance of rotamer III may be explained by steric hindrance between the side chain of Gln-19 and the phenyl ring of Phol-20.

CONCLUSIONS

Evidence has been presented here for an extensive helical structure, which starts at Pro-2 and terminates at Glu-18. Most of this is a regular helix structure except the slight distortions necessary to accommodate the two proline residues. In addition, there is a bend around Gly-11 and Leu-12 that may tilt the axis of the helix but does not reverse the direction of the chain. The Aib-1 N-terminus is not in a helical conformation, and the C-terminal dipeptide exists in a somewhat extended structure. A model consistent with the NMR data is shown in Figure 5.

With the exception of the C-terminal dipeptide and the side chains of Glu-18 and Gln-19, the conformation of alamethicin found here is very similar to the crystal structure. There are, however, several differences between the alamethicin structure in methanol, proposed by Banerjee et al. (1983), and the one reported here. The differences mainly concern the conformation of the segment 10–20. No evidence for a head to head dimer was found in the present study and no NOE connectivity was detected between the Phol-20 ortho protons and the Val-15 α -CH.

The results of this study suggest that alamethicin may not be flexible enough to produce the large changes in conformation drawn by Hall et al. (1984) and Fox and Richards (1982) in their models for ion channel gating. The present results might suggest that the "helix dipole" (Jung et al., 1975; Edmonds, 1985) models are more likely.

ACKNOWLEDGMENTS

We thank the Medical Research Council and Eniricerche spa. We also thank Dr. J. Gagnon for his help with the purification of alamethicin, Dr. G. Taylor and Dr. A. Pastore for help with the molecular graphics and Figure 5, and N. Soffe for his help with the NMR spectrometers.

APPENDIX

Stereospecific Assignments. It was possible to exploit some of the distance constraints imposed by the secondary structure to assign several resonances stereospecifically. For Aib, in a regular helix structure, the methyl substituting the α proton of an L residue, the *pro-R*-methyl, is 2.6–3.0 Å from the NH, while the other β -methyl, the *pro-S*-methyl, is 2.0–2.5 Å from the NH (taking shortest distances to one of the C^β protons.) Usually only a single methyl NOE connectivity appeared in the cross sections corresponding to the Aib NH's. This observation allows stereospecific assignment for the methyls as outlined in Table I.

A series of stereospecific assignments other than those for Aib are also listed in Table I. The Val-9 γ -methyls were stereospecifically assigned by a combination of evidence from intra- and interresidue NOEs. Intraresidue connectivities were detected between the NH resonance and the β proton and γ_1 -methyl (i.e., the low-field one) resonances. The interresidue connectivities of Val-9 (Figures 2 and 3), along with the value of $J_{\text{NH}\alpha}$ (Table III), show a typical pattern for a helical structure (Wüthrich et al., 1984). In particular, the detection of NOEs from the Val-9 β proton to the Aib-10 NH and to Ala-6 α -CH resonances (Figure 3) restricts the possible orientation of the C^β -H bond along a definite direction, pointing to the N-terminus of the molecule. The nearest methyl to the NH is the C^γ_2 methyl (IUPAC-IUB Commission on Biochemical Nomenclature, 1970), *pro-S* in absolute configuration. The value of χ^1 should be around 180°, in agreement with a recent stereospecific assignment of the same groups in helical structures (Zuiderweg et al., 1985). [The apparent discrepancy between our results and those presented in this reference arises from different conventions adopted to define χ^1 for valines (IUPAC-IUB Commission on Biochemical Nomenclature, 1970; Janin et al., 1978).]

The α -proton resonances of Gly-11 were assigned stereospecifically on the basis of their NOESY correlations and coupling constants. The NOE detected between the NH and the high-field α -proton (α_2) resonances of Gly-11 was always greater than that to the α_1 proton. The coupling constants of the Gly-11 spin system were evaluated from simulation of the 1D spectral pattern at 300 MHz. All possible ϕ values were computed (Table V), and the range of solutions was restricted by imposing NOE constraints as outlined in Table V. The corresponding ϕ_{11} values are very close to the typical α_R - and α_L -helix values, depending on the chirality chosen for the α protons. The presence of a right-handed helix structure prior to Gly-11, as well as the conformational continuity next to it (see Structure), is only compatible with the α_R -helix-like value of ϕ_{11} . This defines the stereospecific assignment of the α -proton resonances, as given in Table I.

For the ring protons of Pro-2, the intraresidue NOESY connectivities indicate that the α proton is *cis* to β_1 , whereas the β_2 is closer to γ_1 , which, in turn, is seen to be *cis* to δ_2 . Such a network is consistent with the observed interresidue NOEs arising from the same resonances. By inspection of a model, the assignment of the ring proton resonances can be deduced to be that listed in Table I. The stereospecific assignment for Pro-14 δ protons and Aib-13 β -CH₃ can also be deduced from the observed interresidue NOEs.

Stereospecific assignments of the β -CH₂ protons of the Phol residue for *N*-Ac-Phol have been given previously by Kobayashi and Nagai (1978). Substitution of the *N*-acetyl protecting group with a peptidyl group is not expected to change the chemical shifts significantly (Kobayashi et al., 1981) so their previous assignments are assumed valid here. The ro-

tamer populations, corresponding to the measured $J_{\alpha\beta}$ coupling constants, can then be calculated, as shown in Table VI. Since the relationship between conformer populations and coupling constants for α -amino acids (Pachler, 1964) may be unsuitable for an amino alcohol, the general relationship proposed by Haasnoot et al. (1980) was employed. The results (Table VI) show that only two rotamers account for 90–95% of the conformational distribution.

SUPPLEMENTARY MATERIAL AVAILABLE

NOESY contour plots and cross sections illustrating the stereospecific assignments of Val-9 and Gly-11 (2 pages). Ordering information is given on any current masthead page.

Registry No. Alamethicin, 27061-78-5.

REFERENCES

- Balaram, P. (1983) in *Peptides: Structure and Function* (Hruby, V. J., & Rich, D. M., Eds.) pp 477–486, Pierce Chemical Co., Rockford, IL.
- Banerjee, U., & Chan, S. I. (1983) *Biochemistry* 22, 3709–3713.
- Banerjee, U., Tsui, F., Balasubramanian, T. N., Marshall, G. R., & Chan, S. I. (1983) *J. Mol. Biol.* 165, 757–775.
- Banerjee, U., Zidovetzki, R., Birge, R. R., & Chan, S. I. (1985) *Biochemistry* 24, 7621–7627.
- Barfield, H., Hruby, V. J., & Meraldi, J. P. (1976) *J. Am. Chem. Soc.* 98, 1308–1314.
- Bates, R. G. (1971) *J. Electroanal. Chem. Interfacial Electrochem.* 29, 1–19.
- Bodenhausen, G., & Ernst, R. R. (1982) *J. Am. Chem. Soc.* 104, 1304–1309.
- Boheim, G., & Kolb, H. A. (1978) *J. Membr. Biol.* 38, 151–191.
- Boheim, G., Hanke, W., & Jung, G. (1983) *Biophys. Struct. Mech.* 9, 181–191.
- Bundi, A., & Wüthrich, K. (1979a) *Biopolymers* 18, 285–297.
- Bundi, A., & Wüthrich, K. (1979b) *Biopolymers* 18, 299–311.
- Chothia, C. (1984) *Annu. Rev. Biochem.* 53, 537–572.
- Davis, D. G., & Gisin, B. F. (1981) *FEBS Lett.* 133, 247–251.
- Davis, D. G., & Bax, A. (1985) *J. Am. Chem. Soc.* 107, 2820–2821.
- De Marco, A., Llinas, M., & Wüthrich, K. (1978) *Biopolymers* 17, 637–650.
- Ebina, S., & Wüthrich, K. (1984) *J. Mol. Biol.* 179, 283–288.
- Edmonds, D. T. (1985) *Eur. Biophys. J.* 13, 31–35.
- Fox, R. O., Jr., & Richards, F. M. (1982) *Nature (London)* 300, 325–330.
- Fringeli, U. P., & Fringeli, M. (1979) *Proc. Natl. Acad. Sci. U.S.A.* 76, 3852–3856.
- Gisin, B. F., Kobayashi, S., Davis, D. G., & Hall, J. E. (1977) *Pept. Proc. Am. Pept. Symp.*, 5th, 215–218.
- Gisin, B. F., Davis, D. J., Borowska, Z. K., Hall, J. E., & Kobayashi, S. (1981) *J. Am. Chem. Soc.* 103, 6373–6377.
- Haasnoot, C. A. G., De Leeuw, F. A. A. M., & Altona, C. (1980) *Tetrahedron* 36, 2783–2792.
- Hall, J. E., Vodyanoy, I., Balasubramanian, T. M., & Marshall, G. M. (1984) *Biophys. J.* 45, 233–247.
- Hoult, D. I., & Richards, R. E. (1975) *Proc. R. Soc. London, A* 344, 311–320.
- IUPAC-IUB Commission on Biochemical Nomenclature (1970) *Eur. J. Biochem.* 17, 193–201.
- Janin, J., Wodak, S., Levitt, M., & Maigret, B. (1978) *J. Mol. Biol.* 125, 357–386.
- Jones, T. A. (1978) *J. Appl. Crystallogr.* 11, 268–272.
- Jung, G., Dubishar, N., & Leibfritz, D. (1975) *Eur. J. Biochem.* 54, 395–409.
- Kobayashi, J., & Nagai, U. (1978) *Biopolymers* 17, 2265–2277.
- Kobayashi, J., Higashijima, T., Sekido, S., & Miyazawa, T. (1981) *Int. J. Pept. Protein Res.* 17, 486–494.
- Lau, A. L. Y., & Chan, S. I. (1976) *Biochemistry* 15, 2551–2555.
- Macura, S., Wüthrich, K., & Ernst, R. R. (1982) *J. Magn. Reson.* 46, 269–282.
- Martin, D. R., & Williams, R. J. P. (1976) *Biochem. J.* 153, 181–190.
- Mathew, M. K., & Balaram, P. (1983) *FEBS Lett.* 157, 1–5.
- McMullen, A. I., Marlborough, D. I., & Bayley, P. M. (1971) *FEBS Lett.* 16, 278–280.
- Mueller, P., & Rudin, D. O. (1968) *Nature (London)* 217, 713–719.
- Ohnishi, M., & Urry, D. W. (1969) *Biochem. Biophys. Res. Commun.* 36, 194–202.
- Pachler, K. G. R. (1964) *Spectrochim. Acta* 20, 581–587.
- Pardi, A., Billeter, M., & Wüthrich, K. (1984) *J. Mol. Biol.* 180, 741–751.
- Payne, J. W., Jakes, R., & Hartley, B. S. (1970) *Biochem. J.* 117, 757–766.
- Piantini, U., Sørensen, O. W., & Ernst, R. R. (1982) *J. Am. Chem. Soc.* 104, 6800–6801.
- Richardson, J. S. (1981) *Adv. Protein Chem.* 34, 167–339.
- Shaka, A. J., & Freeman, R. (1983) *J. Magn. Reson.* 51, 169–173.
- States, D. J., Haberkorn, R. A., & Ruben, B. J. (1982) *J. Magn. Reson.* 48, 286–292.
- Wagner, G., & Wüthrich, K. (1982) *J. Mol. Biol.* 155, 347–366.
- Wider, G., Lee, K. M., & Wüthrich, K. (1982) *J. Mol. Biol.* 155, 367–388.
- Wider, G., Hosur, R. V., & Wüthrich, K. (1983) *J. Magn. Reson.* 52, 130–131.
- Wokaun, A., & Ernst, R. R. (1977) *Chem. Phys. Lett.* 52, 407–412.
- Wüthrich, K., Billeter, M., & Braun, W. (1984) *J. Mol. Biol.* 180, 715–740.
- Zuiderweg, E. R. P., Boelens, R., & Kaptein, R. (1985) *Biopolymers* 24, 601–611.